ISSN 1070-3284, Russian Journal of Coordination Chemistry, 2016, Vol. 42, No. 7, pp. 429–435. © Pleiades Publishing, Ltd., 2016.

Two Cadmium(II) Complexes with Polymeric 2D Layer and Discrete Mononuclear Motifs: Syntheses, Crystal Structures, and Fluorescent Properties[1]

P. X. Dai[a, b, *], Q. C. Du[a, b], and H. G. Ge[a, b, *]

[a] *College of Chemistry and Environmental Science, Shaanxi University of Technology, Hanzhong, Shaanxi, 723001 P.R. China*

[b] *Shaanxi Province Key Laboratory of Catalytic Fundamental and Applications, Shaanxi University of Technology, Hanzhong, Shaanxi, 723001 P.R. China*

**e-mail: dpx@iccas.ac.cn; gehg@snut.edu.cn*

Received October 15, 2015

Abstract—Two new 1,3-bi(4-pyridyl)propane-based cadmium(II) complexes, $[Cd(Bpp)_2(Nas)_2]_n$ (**I**) and $[Cd(Bpp)_2(Na)_2(H_2O)_2]$ (**II**) (Bpp = 1,3-bi(4-pyridyl)propane, Nas^- = 2-aminonaphthalene-1-sulfonate, and Na^- = 1-naphthoate) (CIF files CCDC nos. 1429589 (**I**), 1429590 (**II**)) have been hydrothermally synthesized by varying carboxylate- or sulfonate-containing coligands. Structural analyses reveal that, complex **I** with monodentate Nas^- ligands exhibits a two-dimensional (2D) layered motif extended by equatorial Bpp connectors. By contrast, complex **II** modified by monodentate Na^- ligands exhibit discrete mononuclear structure. Althouth the Nas^-/Na^- coligands showed the same monodentate binding modes, the Bpp ligand exhibits bridging or terminal binding modes in **I** and **II**, respectively. So it is obvious that the competitive coordination in the present mixed-ligands system is responsible for the aggregation or dissociation of mononuclear structural units. Furthermore, both of the two compounds are linked to 3D supramolecular architecture by intermolecular C–H···O hydrogen bonding or C–H···π stacking interactions, exhibiting strong fluorescent emissions resulting from the ligand-to-metal or Na^--based intraligand charge transfer at room temperature, which can be hopefully used as fluorescent materials.

DOI: 10.1134/S1070328416070022

INTRODUCTION

Because of their aesthetically fascinating structures of topology [1] and the potential applications such as fluorescent materials [2], magnetic materials [3], selective catalyst [4], gas adsorbents [5], and molecular separation [6], metal organic complexes have been one hot subject of research for many chemists and material scientists. In this aspect, the choice of appropriate ligand is the key to construct complexes with special structure and property. Compared with the rigid ligand, flexible ligand shows better tenability to construct intriguing framework. The incorporating of aliphatic chain between the rigid pyridyl rings increase the flexibility of organic ligand, a series of complexes based on bi(4-pyridyl)alkanes have been reported, including diverse structures from discrete oligomers to high dimensional metal organic frameworks [2, 7–13]. Among of these compounds, bi(4-pyridyl)alkane has displayed two significant features, the organic linkers with variable length exhibit versatile conformations due to free rotation of the C–C σ single bond in the aliphatic chain. On the other hand, bi(4-pyridyl)alkane ligand can act as an organic linker to aggregate metal centers together by bidentate bridging mode with different metallomacrocycles formed by metal ions and bridging ligands, which are increased with increment of the length of aliphatic chain. Obviously, the length of the aliphatic chain plays an key role for the structural motifs of the coordination complexes based on bi(4-pyridyl)alkanes.

Herein, to further investigate the competitive coordination ability of bi(4-pyridyl)alkanes in mixed ligands system, two O-donor-based coligands respectively with functional sulfonate and carboxylate groups, 2-aminonaphthalene-1-sulfonate acid (HNas) and 1-naphthoic acid (HNa), were chosen as fundamentally building blocks to self-assembly with 1,3-bi(4-pyridyl)propane (Bpp) and inorganic cadium(II) salts. Obviously, the particular reason for introducing the two different coligands is that the coordination ability of organic sulfonate ligand to metal ion is generally considered weaker than that of the deprotonated carboxylate group. In the present contribution, two novel complexes, $[Cd(Bpp)_2(Nas)_2]_n$ (**I**) and $[Cd(Bpp)_2(Na)_2(H_2O)_2]$ (**II**) were hydrothermally obtained and structurally

[1] The article is published in the original.

characterized. Despite the Nas^-/Na^- coligands showed the same monodentate binding modes, **I** owns 2D layer motif and **II** exhibits discrete mononuclear structure, both of which are linked to 3D supramolecular architecture by intermolecular C–H···O hydrogen bonding or C–H···π stacking interactions. Furthermore, both compounds exhibit strong fluorescent emissions at room temperature, which primarily resulted from ligand-to-metal or the intraligand electronic transfer ascribed of Na^- anion.

EXPERIMENTAL

Reagents and instruments. HNas and HNa were purchased from Acros and other analytical-grade starting materials were obtained commercially and used as received without further purification. Doubly deionized water was employed for the conventional synthesis. IR spectra were collected in a range of 4000–400 cm^{-1} region on a Nicolet IR-200 spectrometer with KBr pellets. Elemental analyses for C, H and N were determined on a Perkin-Elmer 2400C elemental analyzer. Thermogravimetric analysis (TGA) experiments were carried out on a Shimadzu simultaneous DTG-60A thermal analysis instrument with a heating rate of 10°C min^{-1} from room temperature to 800°C under a nitrogen atmosphere (flow rate 10 mL min^{-1}). Fluorescence spectra of the polycrystalline powder samples of I and II were performed on a Fluorolog-3 fluorescence spectrophotometer from Horiba Jobin Yvon at room temperature.

Synthesis of I. A mixture of HNas (89.3 mg, 0.4 mmol), Bpp (39.6 mg, 0.2 mmol), $CdAc_2 \cdot 2H_2O$ (106.6 mg, 0.4 mmol), NaOH (24.0 mg, 0.6 mmol), and doubly deionized water (12 mL) were sealed in a 23 mL stainless steel vessel. Then the mixture was heated at 140°C for 72 h under autogenous pressure. After the mixture was cooled to room temperature at the rate of 5°C h^{-1}, colorless block-shaped crystals suitable for single-crystal X-ray diffraction analysis were isolated directly, washed with ethanol, and dried in air. The yield was 46% based on Cd salts.

For $C_{46}H_{44}N_6O_6S_2Cd$

anal. calcd., %:	C, 57.95;	H, 4.65;	N, 8.81.
Found, %:	C, 57.92;	H, 4.67;	N, 8.83.

IR (ν, cm^{-1}): 3445 ν(N–H), 3340 ν(N–H), 3046 ν(C–H), 1220 $\nu(SO_3^-)$, 1160 $\nu(SO_3^-)$, 619 $\nu(SO_3^-)$.

Synthesis of II. Pink block-shaped crystals of **II** suitable for single-crystal X-ray diffraction analysis were obtained by adopting the similar procedures to those of **I** only with HNa instead of HNas. The yield was 33% based on Cd salts.

For $C_{48}H_{46}N_4O_6Cd$

anal. calcd., %:	C, 64.97;	H, 5.23;	N, 6.31.
Found, %:	C, 65.15;	H, 5.12;	N, 6.50.

IR (ν, cm^{-1}): 3430 ν(O–H), 3060 ν(C–H), 1607 $\nu_{as}(COO^-)$, 1559 $\nu_{as}(COO^-)$, 1415 $\nu_s(COO^-)$, 1370 $\nu_s(COO^-)$.

X-ray diffraction analysis. Single-crystal X-ray diffraction data for **I** and **II** were collected on a computer-controlled Bruker APEX-II CCD diffractometer equipped with graphite-monochromated MoK_α radiation with radiation wavelength 0.71073 Å by using ω–φ scan mode at room temperature. Semiempirical multiscan absorption corrections were applied using SADABS [14] and the program SAINT [15] was used for integration of the diffraction profiles. Both structures were solved by direct methods and refined with the full-matrix least-squares technique using the SHELXS-97 and SHELXL-97 programs [16]. Anisotropic thermal parameters were assigned to all nonhydrogen atoms. The organic hydrogen atoms were generated geometrically. Details for crystallographic data were listed in Table 1, and selected bond lengths and angles were given in Table 2. Hydrogen-bonding parameters for **I** and **II** were shown in Table 3. Supplementary material has been deposited with the Cambridge Crystallographic Data Centre (nos. 1429589 (**I**) and 1429590 (**II**); deposit@ccdc.cam.ac.uk or http://www.ccdc.cam.ac.uk).

RESULTS AND DISCUSSION

Phase-pure crystals of **I** and **II** were successfully prepared under similar hydrothermal conditions in basic medium. Obviously, the introduction of aqueous NaOH solution is to make HNas/HNa coligands deprotonation and facilitate their coordination with Cd^{2+} ion. Additionally, complexes **I** and **II** are air stable, insoluble in common organic solvents and can retain their crystalline integrity at ambient conditions for a considerable length of time.

In the IR spectra, the weak absorption peaks located at 3445 and 3340 cm^{-1} for **I** could be ascribed to the stretch vibrations of exocyclic amino group of Nas^- anion. By contrast, the O–H stretching vibrations of water molecule lead to a adsorption band centered at 3430 cm^{-1} in **II**. In addition, the weak absorption peaks appeared at 3046 for **I** and 3060 cm^{-1} **II** should be assigned to the C–H stretching vibrations of aromatic ring. An absence of a characteristic band at 1675 cm^{-1} in **II** indicates the complete deprotonation of HNa ligand by NaOH [17], which is consistent with the results of single crystal structure determinations. Furthermore, the adsorption bands at 1220, 1160 and

619 cm^{-1} in **I** is related to stretching and bending vibrations of the sulfonate group from the Nas^- anion [18]. By contrast, complex **II** shows characteristic peaks at 1607, 1559, and 1415, 1370 cm^{-1} for asymmetric (ν_{as}) and symmetric (ν_s) stretching vibrations of carboxylate group. Thus, the results of IR spectra are well agreement with those of crystal structure determinations.

Complex **I** exhibits a coplanar 2D layer bridged by flexible Bpp ligands. The asymmetric unit of **I** consists of one crystallographically independent Cd^{2+} ion, two neutral Bpp ligand and two monodentate Nas^- anion (Fig. 1a). The sole unique Cd^{2+} ion in **I** is hexa-coordinated in a slightly distorted octahedral coordination geometry defined by four equatorial N donors from the pyridyl group of four neutral Bpp ligands and two axially sulfonate O atoms from Nas^- anions. The Cd–O and Cd–N distances are in the region of 2.287 to 2.427 Å (Table 2), falling into the normal range of Cd(II) complexes derived from mixed carboxylate and/or pyridyl ligands [19–20]. It is considerable that the bond length of the axial Cd(1)–O(1) is 0.10 Å longer than those of Cd–O and Cd–N distances. The Bpp entity adopts a bidentate bridging mode, and the Nas^- anion exhibits a monodentate binding mode to complete the coordination sphere of the central Cd^{2+} ion.

As shown in Fig. 1b, each Cd^{2+} ion in **I** is infinitely extended by four equatorial bpp ligands in a bidentate bridging mode, leading to macrocyclic $\{Cd_4(Bpp)_4\}^{2+}$ subunit-based 2D layer. Adjacent 2D layers of **I** are linked together to form 3D supramolecular architecture by interlayer C–H···O weak hydrogen bonding interactions between the pyridyl rings of Bpp ligands and sulfonate groups of Nas^- anions (Fig. 1c). The distances of H and C atoms to the acceptor O atom from sulfonate moiety of adjacent Nas^- anion are 2.43 and 3.189(9) Å, respectively, and the involved angle (angle CHO) is 138° (Table 3).

Complex **II** with the formula of $[Cd(Bpp)_2(Na)_2(H_2O)_2]$ exhibits a centrosymmetric mononuclear structure. As shown in Fig. 2a, the asymmetric unit of **II** contains a half of crystallographically independent Cd(II) site, one neutral Bpp ligand, one monodentate Na^- anion and one coordinated water molecule. The unique Cd^{2+} ion is six-coordinated by four O atoms from two Na^- anions and two water molecules and two N atom from two Bpp ligands, forming a slightly distorted CdO_4N_2 octahedral geometry. All the bond distances and angles around Cd^{2+} ion fall into the normal range (Table 2) and are comparable to those Cd(II) complexes based on mixed carboxylate and/or pyridyl ligands [19–20]. Different from the bidentate bridging mode in **I**, the Bpp entity adopts a monodentate binding mode to isolate the mononuclear unit, and the Na^- anion also exhibits a monodentate coordination mode to complete the coordination sphere of the central Cd^{2+} ion. Moreover, the separation between the central Cd^{2+} ion and the N atom in **II** is slightly longer than that in **I**, which may be ascribed to different coordination modes of the Bpp ligands. Furthermore, the existence of intramolecular O(3)–H(3*B*)···O(2) hydrogen bonding interaction is helpful to consolidate the mononuclear entity of complex **II**. The distances of H and O(H_2O) atoms to the acceptor O(COO^-) atom from sulfonate moiety of adjacent Nas^- anion are 1.86 and 2.702(4) Å, respectively, and the involved angle (angle CHO) is 170° (Table 3).

As shown in Fig. 2b, the adjacent discrete mononuclear $[Cd(Bpp)_2(Na)_2(H_2O)_2]$ molecules are arranged into a 1D chain by the O(3)–H(3*A*)···N(2) strong hydrogen bonding interaction. The separations

Table 1. Crystallographic data and structure refinement summary for **I** and **II**

Parameter	Value	
	I	**II**
Formula weight	953.39	443.64
Crystal size, mm	0.24 × 0.18 × 0.16	0.34 × 0.24 × 0.15
Crystal system	Orthorhombic	Monoclinic
Space group	$Pna2_1$	$P2_1/n$
a, Å	23.9851(14)	11.1921(15)
b, Å	10.9632(7)	16.185(2)
c, Å	16.6508(10)	11.8837(16)
β, deg	90	104.272(2)
V, $Å^3$	4378.4(5)	2086.3(5)
Z	4	4
ρ_{calcd}, g/cm^3	1.446	1.412
μ_{Mo}, mm^{-1}	0.650	0.578
$F(000)$	1960	916
θ Range, deg	2.04–25.03	2.17–25.01
Range of reflection indices	$-18 \leqslant h \leqslant 28$, $-13 \leqslant k \leqslant 13$, $-19 \leqslant l \leqslant 19$	$-13 \leqslant h \leqslant 13$, $-19 \leqslant k \leqslant 13$, $-14 \leqslant l \leqslant 13$
Reflections collected/unique	22879/7732	11177/3676
R_{int}	0.0311	0.0252
Parameters	550	268
GOOF on F^2	1.025	1.036
R ($I > 2\sigma(I)$)*	$R_1 = 0.0426$, $wR_2 = 0.1113$	$R_1 = 0.0270$, $wR_2 = 0.0646$
R (all reflections)*	0.0577/0.1215	0.0424/0.0691
$\Delta\rho_{max}/\Delta\rho_{min}$, e $Å^{-3}$	0.758/–0.335	0.161/–0.271

* $R_1 = \Sigma(||F_o| - |F_c||)/\Sigma|F_o|$, $wR_2 = [\Sigma w(|F_o|^2 - |F_c|^2)^2/\Sigma w(F_o^2)]^{1/2}$.

Table 2. Selected bond lengths (Å) and angles (deg) for **I** and **II***

Bond	*d*, Å	Bond	*d*, Å
		I	
Cd(1)–N(3)	2.287(5)	Cd(1)–O(4)	2.339(4)
Cd(1)–N(1)	2.304(5)	Cd(1)–N(2)^{ii}	2.344(4)
Cd(1)–N(4)^{i}	2.329(5)	Cd(1)–O(1)	2.427(4)
		II	
Cd(1)–O(1)	2.278(5)	Cd(1)–O(3)	2.344(3)
Cd(1)–N(1)	2.344(3)		
Angle	ω, deg	Angle	ω, deg
		I	
N(1)Cd(1)O(1)	89.73(15)	N(1)Cd(1)(4)	94.53(16)
N(3)Cd(1)O(4)	89.90(17)	N(3)Cd(1)O(1)	85.77(16)
N(1)Cd(1)N(4)^{i}	87.27(18)	N(4)^{i}Cd(1)O(1)	91.50(16)
N(3)Cd(1)N(4)^{i}	90.53(17)	O(4)Cd(1)N(2)^{ii}	95.87(19)
N(4)^{i}Cd(1)O(4)	86.9(2)	N(1)Cd(1)N(2)^{ii}	96.75(17)
N(3)Cd(1)N(2)^{ii}	85.21(16)	N(2)^{ii}Cd(1)O(1)	85.45(15)
		II	
O(1)^{i}Cd(1)N(1)	87.12(7)	O(3)Cd(1)N(1)	89.34(6)
O(1)^{i}Cd(1)O(3)	86.07(6)	O(3)^{i}Cd(1)N(1)	90.66(6)
O(1)Cd(1)O(3)	93.93(6)	O(1)Cd(1)N(1)	92.88(7)

* Symmetry codes: ^{i} $x + 1/2, -y + 3/2, z$; ^{ii} $x - 1/2, -y + 1/2, z$ (**I**); ^{i} $-x, -y, 1 - z$ (**II**).

Table 3. Hydrogen bond lengths (Å) and bond angles (deg) for **I** and **II***

Contact D–H···A	Distance, Å			Angle D–H···A, deg
	D–H	H···A	D···A	
		I		
C(17)–H(17)···O(5)^{i}	0.93	2.43	3.189(9)	138
		II		
(intra)O(3)–H(3*B*)···O(2)^{ii}	0.85	1.86	2.702(4)	170
O(3)–H(3*A*)···N(2)^{i}	0.85	1.98	2.823(3)	175

* Symmetry codes: ^{i} $1 - x, 1 - y, z + 1/2$ (**I**); ^{i} $x - 1, y, z - 1$; ^{ii} $-x, -y, 1 - z$ (**II**).

between O (donor) and N (acceptor) and O–N···O angle is 2.823(3) Å and 175°, respectively. Moreover, the adjacent 1D chains are linked together by weak C(13)–H(13)···π and C(16)–H(16)···π stacking interactions between bpp ligands and benzene rings of Na^- anions, leading to the 3D supramolecular architecture of **II** (Fig. 2c). The distances of H to the center of benzene ring (H···Cd) are 2.633(6) and 2.928(5) Å, the angle of HCCd are 146° and 129°, respectively.

Under the competitive coordination of the present mixed ligands, although the Nas^-/Na^- coligands in **I** and **II** exhibit the same binding modes (monodentate coordination mode), the Bpp ligand exhibits different coordination modes: bidentate bridging for **I** and monodentate terminal binding modes for **II**. Apparently, the competitive coordination governs the aggregation or dissociation of the mononuclear structure.

To explore their thermal stability, TGA experiments of **I** and **II** were carried out and the results were presented in Fig. 3. As a result, I can be thermally stable up to 256°C and is followed by a continuous two-step weight-loss stage between 256 and 503°C. The obvious weight-loss stage is corresponding to the broken of the polymeric structure and the decomposition of the mixed ligands. The remained substance beyond 503°C is calculated to be CdO (obsd. 14.7%, calcd.

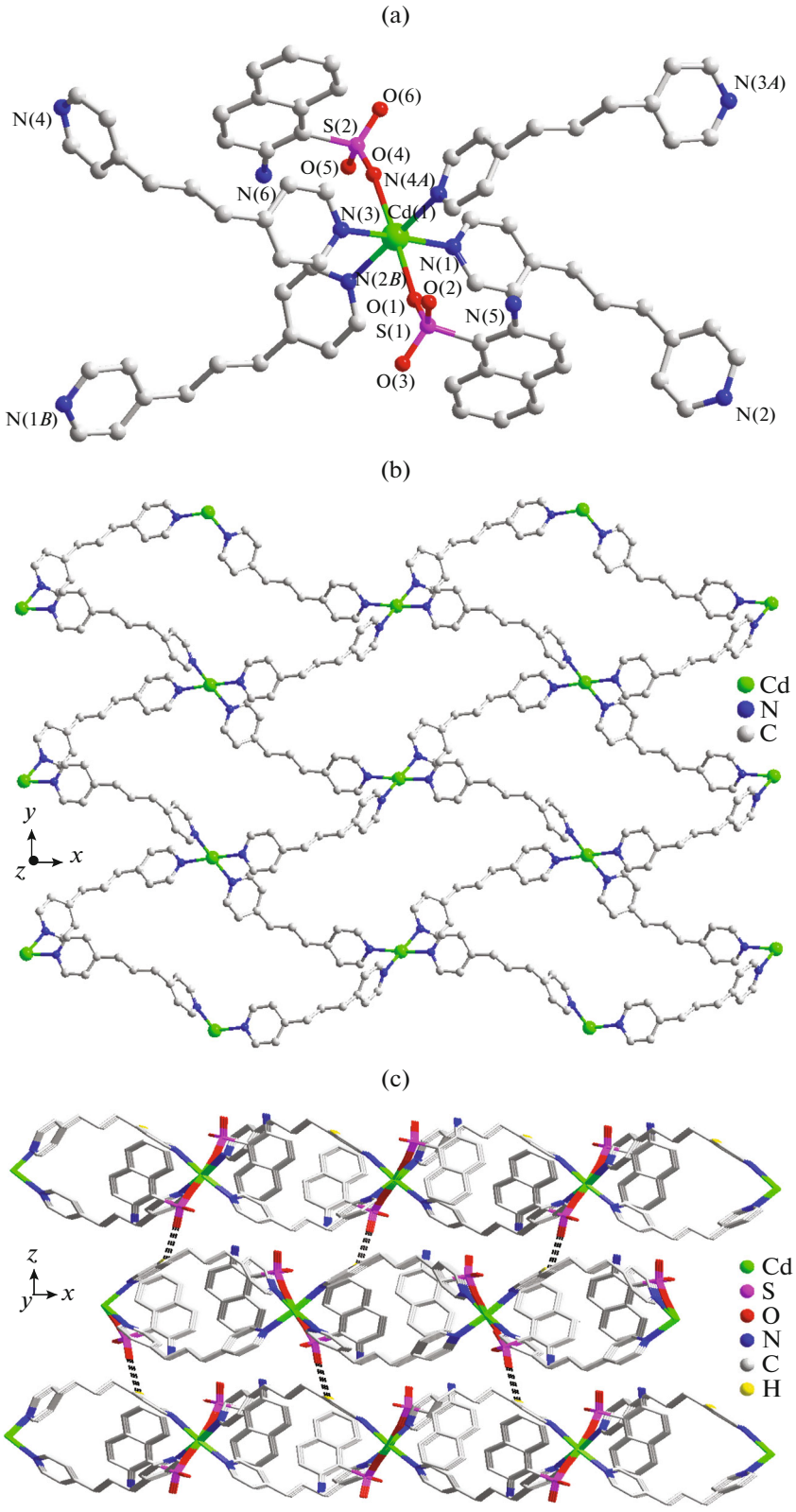

Fig. 1. Local coordination environment of Cd^{2+} ion in **I** (a) (hydrogen atoms were omitted for clarity. Symmetry codes: $A = x + 1/2, -y + 3/2$; $B = x - 1/2, -y + 1/2, z$); 2D network of **I** with Cd^{2+} ion extended by ditopic Bpp connectors (b) (the terminal Nas^{-} ligands were omitted for clarity); 3D supramolecular architecture of **I** by interlayer C(17)–H(17)···O(5) interactions (c) (only H atoms involved in hydrogen bonds were included).

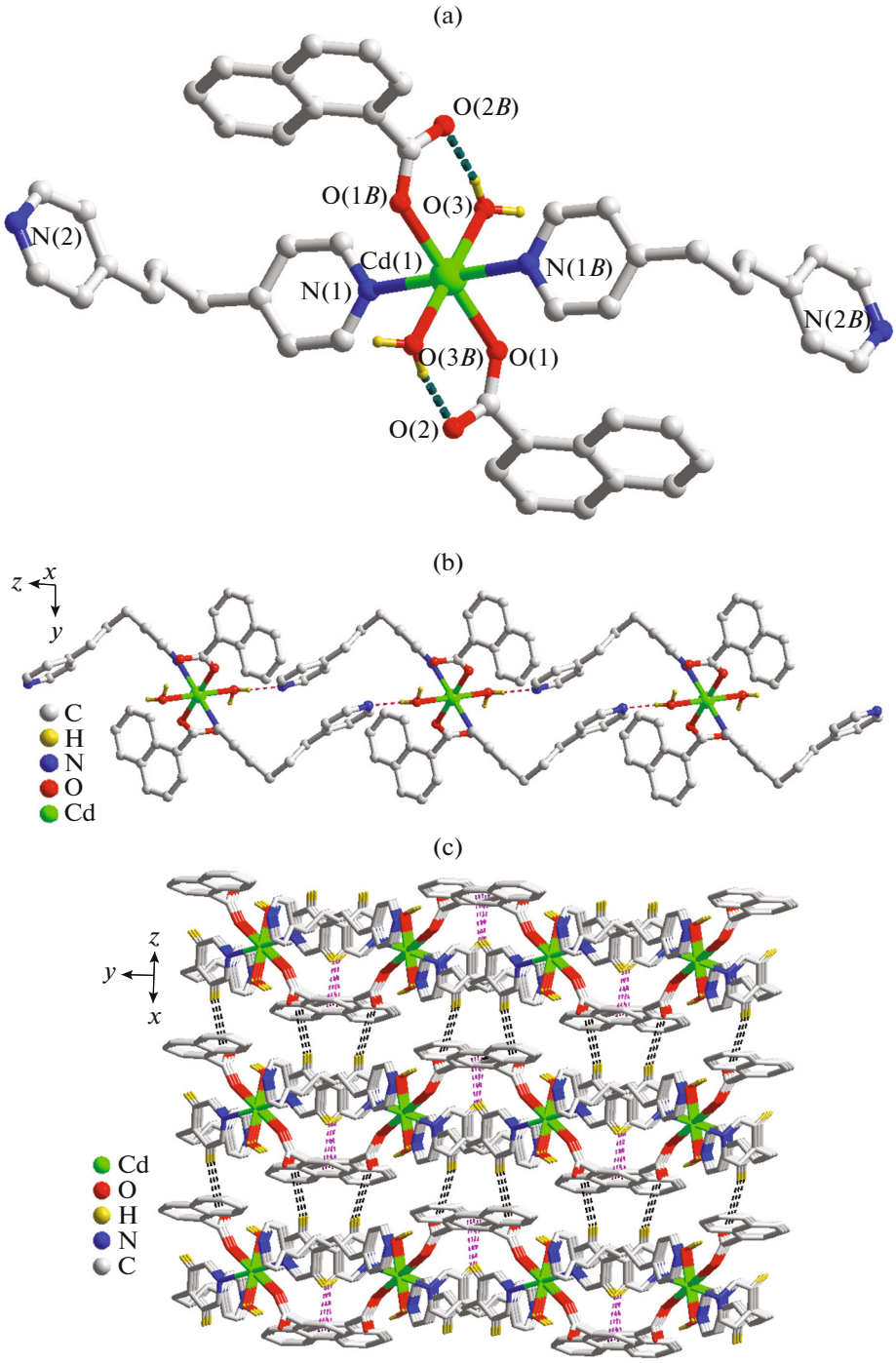

Fig. 2. Mononuclear structure of **II** (a) (hydrogen atoms were omitted for clarity. Symmetry codes: $B = -x, -y, -z + 1$); 1D chain of **II** connected by intermolecular O(3)–H(3*A*)···N(2) hydrogen bonds interactions (b) (only H atoms involved in hydrogen bonds were included); 3D supramolecular architecture of **II** formed by C(13)–H(13)···π and C(16)–H(16)···π stacking interactions (c) (only H atoms involved in hydrogen bonds were included).

13.4%). For **II**, from 46 to 464°C, the only slow and complicated weight loss can be observed (calcd. 85.5%, obsd. 84.1%), ascribing to the loss of coordinated water molecule and Bpp ligand and Na^- anions. The remaining CdO fragment is stable upon further heating until it ends at 800°C.

The solid-state emission spectra at room temperature were examined, together with the free HNas and HNa ligands for comparison. As shown in Fig. 4, upon excitation at 327 nm, complex **I** display blue photoluminescence with maximum emission at 409 nm. By contrast, a strong emission at 402 nm is observed in **II**

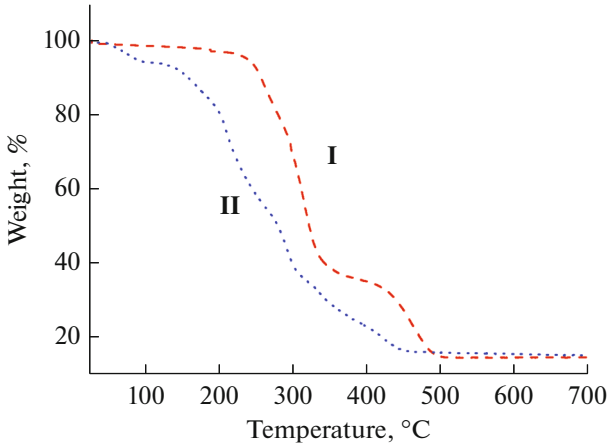

Fig. 3. TG curves for **I** and **II**.

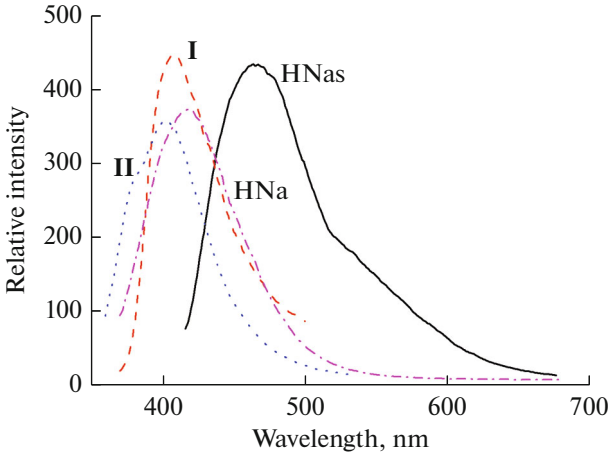

Fig. 4. Solid-state emissions of **I** and **II** at room temperature.

upon excitation at 334 nm. Under comparable experimental conditions, free HNas species show a broad maximum at 462 nm (λ_{ex} = 349 nm) and the HNa ligand gives strong emission occurs at 421 (λ_{ex} = 370 nm). Therefore, observed luminescence for **I** should be ascribed to the ligand-to-metal charge-transfer (LMCT) and the emission for **II** is due to intraligand electron-transfer. The slight blue shift of the emission wavelength is probably resulted from the energy gap between the intraligand molecular orbitals decrease because of the deprotonation of HNas/HNa and the coordination behavior of the Na^-/Nas^- to Cd^{2+} ion [21].

In summary, two novel 1,3-bi(4-pyridyl)propane-derived Cd(II) complexes possessing 2D layer and discrete mononuclear structure modulated by carboxylate- or sulfonate-containing coligands have been hydrothermally synthesized and structurally characterized. Structural analysis reveals that the competitive coordination in the present mixed-ligands system play key roles in governing the dimension of the comparable complexes. Ascribing into the ligand-to-metal or Na^--based intraligand charge transfer, both the two complexes exhibit strong fluorescent emissions, suggest their potential applications as luminescent materials.

ACKNOWLEDGMENTS

This present work was supported by the National Natural Science Foundation of China (21373132) and the Science Foundation of Shaanxi University of Technology (SLGQD13-4), which are gratefully acknowledged.

REFERENCES

1. Dong, M.M., He, L.L., Fan., Y.J., et al., *Cryst. Growth Des.*, 2013, vol. 13, no. 8, p. 3353.
2. Li, M., Yao, Y., Ding, J., et al., *Inorg. Chem.*, 2015, vol. 54, no. 4, p. 1346.
3. Zhang, N., Zhang, J.Y., Jia, Q.X., et al., *RSC Adv.*, 2015, vol. 5, no. 87, p. 70772.
4. Hanson, S.K. and Baker, R.T., *Acc. Chem. Res.*, 2015, vol. 48, no. 7, p. 2037.
5. Marco-Lozar, J.P., Juan-Juan, J., Suarez-Garcia, F., et al., *Int. J. Hydrogen Energy*, 2012, vol. 37, no. 3, p. 2370.
6. Li, Z.J., Yao, J., Tao, Q., et al., *Inorg. Chem.*, 2013, vol. 52, no. 20, p. 11694.
7. Xu, B., Guo, S., Li, Z.W., et al., *Z. Anorg. Allg. Chem.*, 2015, vol. 641, no. 7, p. 1311.
8. Li, B.Y., Li, G.H., Liu, D., et al., *CrystEngComm.*, 2011, vol. 13, no. 5, p. 1291.
9. Ma, X., Cha, Y.E., Zhao, K., et al., *J. Coord. Chem.*, 2012, vol. 65, no. 14, p. 2500.
10. Lee, T.W., Lau, J.P.K., and Wong, W.T., *Polyhedron*, 2004, vol. 23, no. 6, p. 999.
11. Fu, Z.Y., Hu, S.M., Dai, J.C., et al., *Eur. J. Inorg. Chem.*, 2003, no. 14, p. 2670.
12. Zhang, L.J., Xu, D.H., Zhou, Y.S., et al., *J. Coord. Chem.*, 2012, vol. 65, no. 17, p. 3028.
13. Dias de Souza, N.L.G., Garcia, H.C., de Souza, M.C., et al., *J. Mol. Struct.*, 2015, vol. 1085, p. 21.
14. Sheldrick, G.M., *SADABS, Program for Empirical Absorption Correction of Area Detector Data*, Göttingen: Univ. of Göttingen, 1996.
15. *SAINT, Software Reference Manual*, Madison (WI, USA): Bruker AXS, 1998.
16. Sheldrick, G.M., *SHELXTL, Structure Determination Software Programs*, Madison (WI, USA): Bruker Analytical X-ray System, Inc., 2001.
17. Bellamy, L.J., *The Infra-Red Spectra of Complex Molecules*, New York: Wiley, 1958.
18. Yang, E.C., Dai, P.X., Wang, X.G., et al., *Z. Anorg. Allg. Chem.*, 2007, vol. 633, no. 4, p. 615.
19. Cao, L.H., Wei, Y.L., Yang, Y., et al., *Cryst. Growth Des.*, 2014, vol. 14, no. 4, p. 1827.
20. Dai, P.X., Yang, E.C., and Zhao, X.J., *Russ. J. Coord. Chem.*, 2015, vol. 41, no. 1, p. 16.
21. Huang, W.H., Wang, Y.Y., Zhang, Y.N., et al., *Inorg. Chim. Acta*, 2015, vol. 433, p. 52.